

The 2008 May burst activation of SGR 1627–41

P. Esposito,^{1,2*} G. L. Israel,³ S. Zane,⁴ F. Senziani,^{2,5} R. L. C. Starling,⁶ N. Rea,⁷
D. M. Palmer,⁸ N. Gehrels,⁹ A. Tiengo,² A. De Luca,^{1,2,5} D. Götz,¹⁰ S. Mereghetti,²
P. Romano,¹¹ T. Sakamoto,⁸ S. D. Barthelmy,⁸ L. Stella,³ R. Turolla,^{4,12} M. Feroci¹³
and V. Mangano¹¹

¹Dipartimento di Fisica Nucleare e Teorica and INFN-Pavia, Università degli Studi di Pavia, via A. Bassi 6, 27100 Pavia, Italy

²INAF/Istituto di Astrofisica Spaziale e Fisica Cosmica – Milano, via E. Bassini 15, 20133 Milano, Italy

³INAF/Osservatorio Astronomico di Roma, via Frascati 33, 00040 Monteporzio Catone, Italy

⁴Mullard Space Science Laboratory, University College London, Holmbury St. Mary, Dorking, Surrey RH5 6NT

⁵IUSS – Istituto Universitario di Studi Superiori, viale Lungo Ticino Sforza 56, 27100 Pavia, Italy

⁶Department of Physics and Astronomy, University of Leicester, Leicester LE1 7RH

⁷Astronomical Institute Anton Pannekoek, University of Amsterdam, Kruislaan 403, 1098 SJ Amsterdam, the Netherlands

⁸Los Alamos National Laboratory, Los Alamos, NM 87545, USA

⁹NASA Goddard Space Flight Center, Greenbelt, Maryland 20771, USA

¹⁰CEA Saclay, DSM/Irfu/Service d'Astrophysique, Orme des Merisiers, Bât. 709, 91191 Gif sur Yvette, France

¹¹INAF/Istituto di Astrofisica Spaziale e Fisica Cosmica – Palermo, via U. La Malfa 163, 90146 Palermo, Italy

¹²Dipartimento di Fisica, Università degli Studi di Padova, via F. Marzolo 8, 35131 Padova, Italy

¹³INAF/Istituto di Astrofisica Spaziale e Fisica Cosmica – Roma, via Fosso del Cavaliere 100, 00133 Roma, Italy

Accepted 2008 July 10. Received 2008 July 10; in original form 2008 June 18

ABSTRACT

In 2008 May, the soft gamma-ray repeater (SGR) SGR 1627–41 resumed its bursting activity after nearly a decade of quiescence. After detection of a bright burst, *Swift* pointed its X-ray telescope in the direction of the source in less than five hours and followed it for over five weeks. In this Letter, we present an analysis of the data from these *Swift* observations and an *XMM-Newton* one performed when SGR 1627–41 was still in a quiescent state. The analysis of the bursts detected with *Swift*/Burst Alert Telescope shows that their temporal and spectral properties are similar to those found in previous observations of SGR 1627–41 and other SGRs. The maximum peak luminosity of the bursts was $\sim 2 \times 10^{41}$ erg s⁻¹. Our data show that the outburst was accompanied by a fast flux enhancement and by a hardening of the spectrum with respect to the persistent emission.

Key words: stars: neutron – X-rays: bursts – X-rays: individual: SGR 1627–41.

1 INTRODUCTION

The soft gamma-ray repeater (SGR) SGR 1627–41 is likely to host a ‘magnetar’, that is, an isolated neutron star believed to have an extremely strong magnetic field ($B \sim 10^{14}$ – 10^{15} G) powering their bright X-ray emission and peculiar bursting activity (e.g. Mereghetti 2008). Several magnetars, including SGR 1627–41, have been observed to emit short bursts (<1 s) in the hard X/soft gamma-ray band, with characteristic peak luminosities of the order of $\sim 10^{39}$ – 10^{41} erg s⁻¹. Besides short bursts, SGRs are known to emit intermediate and giant flares, with typical durations of 0.5–500 s, during which luminosities up to $\sim 10^{47}$ erg s⁻¹ can be achieved.

SGR 1627–41 was discovered in 1998 by the *Compton Gamma Ray Observatory* because of the intense bursts it emitted at the time (Kouveliotou et al. 1998). These bursts, more than a hundred in six weeks, were also observed by other X-ray satellites (Feroci

et al. 1998; Hurley et al. 1999; Mazets et al. 1999; Smith, Bradt & Levine 1999; Woods et al. 1999). Soon after the discovery of the bursts, the persistent X-ray emission of this SGR was detected by *BeppoSAX* at a luminosity of $\sim 10^{35}$ erg s⁻¹ (assuming a distance to the source of 11 kpc; Corbel et al. 1999). The quiescent spectrum was well modelled by an absorbed power law ($N_{\text{H}} \approx 8 \times 10^{22}$ cm⁻² and photon index $\Gamma \approx 2.5$; Woods et al. 1999). No further bursting activity has been reported since then, but several X-ray satellites observed the X-ray persistent counterpart of SGR 1627–41 in the past 10 yr (Kouveliotou et al. 2003; Mereghetti et al. 2006). Since its discovery, this persistent emission showed a slow luminosity decay from about 10^{35} to 10^{33} erg s⁻¹, the lowest value ever observed for an SGR, and a spectral softening from $\Gamma \approx 2$ to 4 (Kouveliotou et al. 2003; Mereghetti et al. 2006). The post-burst cooling trend seen in X-rays is peculiar among SGRs; rather it resembles the behaviour of transient anomalous X-ray pulsars (AXPs), a subclass of the magnetar family.

Here, we report on the last observation of SGR 1627–41 performed at the end of the 10-yr long stretch of quiescence and on the

*E-mail: paoloesp@iasf-milano.inaf.it

burst re-activation of the source on 2008 May 28 (Golenetskii et al. 2008; Palmer et al. 2008; Woods et al. 2008a).

2 THE 2008 FEBRUARY XMM–NEWTON OBSERVATION

The last *XMM–Newton* (Jansen et al. 2001) observation of SGR 1627–41 before the 2008 May re-activation was carried out on 2008 February 12 and 13 and lasted about 80 ks. The EPIC pn and MOS cameras (sensitive in the 0.1–15 keV range) were operated in Full Frame mode with the medium optical filter. The data were processed using version 7.1.0 of the *XMM–Newton* Science Analysis Software (sas). We selected events with patterns 0–4 and 0–12 for the pn and the MOS cameras, respectively. The data were filtered to reject intervals with soft-proton flares, reducing the net exposure time to 49.3 ks for the pn detector, 68.3 ks for the MOS 1, and 69.4 ks for the MOS 2.

Source spectra were accumulated for each camera from circular regions with a 25 arcsec radius. The background counts were selected from a 70×150 arcsec² box centred at RA = $16^{\text{h}}36^{\text{m}}01^{\text{s}}.4$, Dec. = $-47^{\circ}34'27''.6$. About 330 counts above the background were collected from SGR 1627–41 by the pn between 2 and 10 keV, 150 by the MOS 1, and 160 by the MOS 2. Spectral redistribution matrices and ancillary response files were generated using the sas tasks RMFGEN and ARFGEN. The spectral fitting was performed using the xSPEC fitting package version 12.4. The data were grouped so as to have at least 20 counts per energy bin and the spectra from the MOS 1, MOS 2 and pn in the 2–10 keV range were fitted simultaneously (spectral channels that have energies below 2 keV were ignored, owing to the very low signal-to-noise ratio). We fit an absorbed power-law model and obtained the following best-fitting parameters [$\chi^2_r = 0.98$ for 42 degrees of freedom (d.o.f.)]: absorption $N_{\text{H}} = (10 \pm 2) \times 10^{22}$ cm⁻² and photon index $\Gamma = 3.3^{+0.6}_{-0.4}$ (hereafter all errors are at 1σ confidence level). The observed 2–10 keV flux was $(6 \pm 2) \times 10^{-14}$ erg cm⁻² s⁻¹. For comparison with previous work (Kouveliotou et al. 2003; Mereghetti et al. 2006), we also fit the data keeping the absorption column fixed at $N_{\text{H}} = 9 \times 10^{22}$ cm⁻², obtaining a similar photon index $\Gamma = 3.0 \pm 0.2$ and a flux of $(6 \pm 1) \times 10^{-14}$ erg cm⁻² s⁻¹. This value (plotted in Fig. 1) hints at a further luminosity decrease since the previous *XMM–Newton* observations (September 2004; Mereghetti et al. 2006).

3 SWIFT OBSERVATIONS AND DATA ANALYSIS

Swift (Gehrels et al. 2004) was specifically designed to study gamma-ray bursts (GRBs) and their afterglows, and its payload includes a wide-field instrument, the Burst Alert Telescope (BAT; Barthelmy et al. 2005), and two narrow-field instruments, the X-Ray Telescope (XRT; Burrows et al. 2005) and the Ultraviolet/Optical Telescope (UVOT; Roming et al. 2005). In this section, we report on the results obtained from our analysis of the *Swift* BAT and XRT observations of SGR 1627–41 performed since its 2008 May re-activation. Given the extremely large optical extinction inferred from the X-ray absorption of the SGR 1627–41 spectrum ($A_V > 40$ mag; Wachter et al. 2004), the UVOT instrument cannot provide meaningful constraints on the ultraviolet/optical emission of SGR 1627–41.

3.1 Burst Alert Telescope data – bursting emission

The coded mask gamma-ray (15–150 keV) BAT instrument spends a large fraction of its time waiting for the occurrence of a GRB in

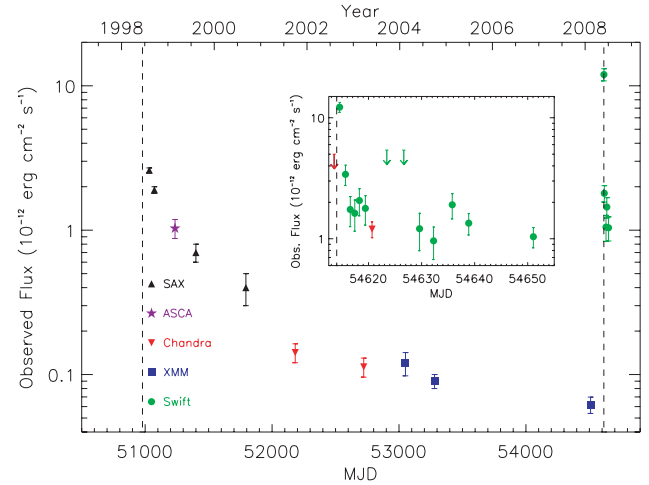


Figure 1. Long-term light curve of SGR 1627–41 based on data from different satellites (updated from Mereghetti et al. 2006). The vertical dashed lines indicate the onset of the two burst-active periods of the source. The inset shows in detail the light curve around the 2008 reactivation, using also *Chandra* data from Tiengo et al. (2008) and Woods et al. (2008b). The down-arrows indicate upper limits at 3σ confidence level.

its field of view (FOV). Whenever a GRB or an interesting hard X-ray transient is detected, information for individual photons is sent to the ground in order to have the maximum energy and time-resolution (event data). If no GRB is detected, the onboard software accumulates the detector count map in 80-channel histograms with a typical integration time of ~ 5 min (survey data). In this mode, continuous full-detector count rate information is available in four energy bands at 64-ms resolution, providing a light curve for bright variable sources in the FOV.

On 2008 May 28 at 08:21:43 UT, BAT triggered on and localized a bright burst from SGR 1627–41 (Palmer et al. 2008). Another bright burst was detected at 09:53:00 UT and was followed by tens of bursts extending to at least 10:25:54 UT (see Fig. 2). Due to the non-continuous coverage, the net exposure time spent by BAT on the source was ~ 3.4 ks. In this section, we present the study of bursts detected when event data were available (~ 2.3 ks).

The data reduction was performed using version 2.8 of the standard *Swift*/BAT analysis software distributed within FTOOLS under the HEASOFT package (version 6.4.0). For each event file, the background-subtracted counts of the source were extracted from the detector pixels illuminated by the source by using the mask-weighting technique. Light curves in the 15–50 keV band showing the bursting activity were produced. For each burst, a spectrum of the entire bursting time interval was extracted.

We identified in the BAT data eight bursts with more than 500 counts in the 15–50 keV energy range. Their spectra were fitted well by an optically thin thermal bremsstrahlung (OTTB) model with temperatures ranging from about 10 to 70 keV and are overall similar to those detected during the previous outburst of SGR 1627–41 as well as the outbursts from other SGRs (Aptekar et al. 2001).

The main problem with the OTTB model is that, while it generally provides good fits to the spectra of SGR bursts in the hard X-rays ($\gtrsim 15$ keV), it tends to overestimate the flux at low energies when broad-band data are available (e.g. Feroci et al. 2004; Olive et al. 2004). Among numerous possible spectral models (see Israel et al. 2008, for a review), we tested the double blackbody (2BB) model that was successfully applied to the SGR bursting emission over broad energy ranges (e.g. Feroci et al. 2004; Olive

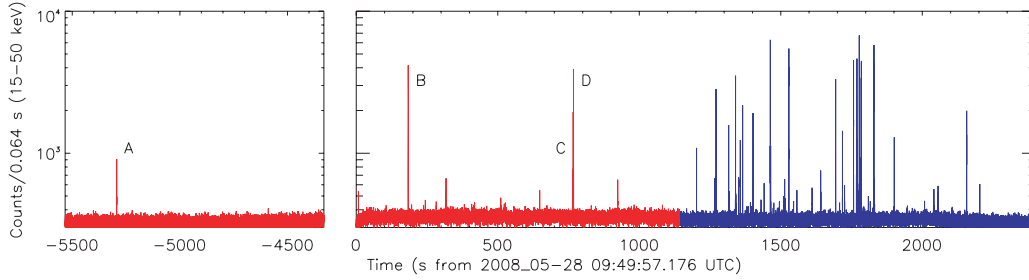


Figure 2. The time-line of the bursts detected by the *Swift* BAT (generated onboard, see Section 3.1). The portion plotted in red corresponds to the temporal range for which event data were available; for the portion in blue only rate and survey data were distributed.

et al. 2004; Nakagawa et al. 2007; Israel et al. 2008). In the case of SGR 1627–41, the 2BB model yielded a good description of the burst spectra as well (even though the additional free parameters with respect to the OTTB model were not statistically required); in Table 1, we show the spectral results for the brightest events. Similar to previous studies, our spectral fits show the presence of a ‘cold’ blackbody with $kT_1 \approx 4$ keV and emitting radius $R_1 \approx 30$ km and a hotter blackbody, with $kT_2 \approx 10$ keV and $R_2 \approx 4$ km.

For these bright bursts, we also produced the spectra corresponding to the rise, peak, and decay phases. The maximum luminosity detected in the SGR 1627–41 data set was $\sim 2 \times 10^{41}$ erg s $^{-1}$ (burst B, peak phase; in particular, the hard blackbody component, with $kT_2 \simeq 11$ keV and radius $R_2 \simeq 8$ km, reached a luminosity of $\sim 10^{41}$ erg s $^{-1}$). Small variations with time were detected, though all the spectra are consistent with the model parameters of the corresponding time-averaged spectrum (see Table 1) simply re-scaled in normalization (to account for the luminosity evolution during the burst). The results of this analysis are reported in Fig. 3 where the two blackbody equivalent surfaces are shown as a function of their temperatures (only time-resolved spectra with well-constrained fitting parameter values are shown). For comparison, we also report the corresponding measurements obtained for the intense ‘burst forest’ emitted by SGR 1900+14 on 2006 March 29 and observed by BAT (Israel et al. 2008). Despite the small number of photons detected in the SGR 1627–41 bursts, their spectral properties are in good agreement with those of SGR 1900+14.

We also searched the data for a persistent emission from SGR 1627–41 during all the non-bursting intervals. For each event file, an image was generated excluding the burst time intervals and the `BATCELLDETECT` tool was run. We investigated two time intervals, the first one (see Fig. 2) ranging from time $t = -5533$ to -4331 s (net exposure time 1201 s) and the second one from $t = 0$ to 1146 s (net exposure 1140 s). In both cases, we found no significant emission; the 3σ upper limits on the flux in the 15–50 keV band for the above quoted intervals are 10^{-9} and 4×10^{-10} erg cm $^{-2}$ s $^{-1}$, respectively (the large difference is due to the coded fraction at which the source was observed in the two cases).

Table 1. Spectral fit results (in the 15–100 keV range) of the bright bursts detected by *Swift*/BAT (see Fig. 2) for the 2BB model. We assume a distance to the source of 11 kpc.

Burst	Net counts	Duration (s)	kT_1 (keV)	R_1 (km)	L_1^a (erg s $^{-1}$)	kT_2 (keV)	R_2 (km)	L_2^a (erg s $^{-1}$)	Fluence (erg cm $^{-2}$)	χ_r^2 (d.o.f.)
A	11 802	0.110	3.8 ± 0.7	35_{-12}^{+26}	3.2×10^{40}	8.4 ± 0.9	5 ± 2	1.6×10^{40}	2.0×10^{-7}	0.90 (34)
B	20 595	0.135	$4.0_{-0.4}^{+0.5}$	30_{-7}^{+10}	3.1×10^{40}	$10.7_{-0.5}^{+0.7}$	3.9 ± 0.6	2.6×10^{40}	3.5×10^{-7}	0.91 (34)
C	3704	0.018	$3.9_{-0.7}^{+0.8}$	34_{-12}^{+22}	3.6×10^{40}	11_{-1}^{+2}	4 ± 1	4×10^{40}	0.6×10^{-7}	1.22 (34)
D	10 497	0.250	4.4 ± 0.5	15_{-3}^{+4}	1.1×10^{40}	10 ± 1	$2.0_{-0.7}^{+0.9}$	0.5×10^{40}	1.7×10^{-7}	1.07 (34)

^aBolometric luminosity of the first/second blackbody.

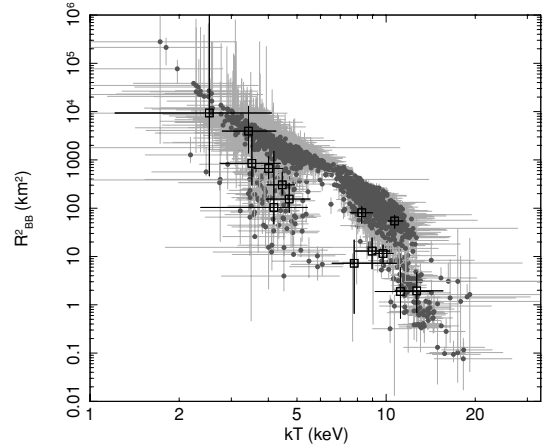


Figure 3. Square of radii for the 2BB model as a function of the corresponding temperatures for the time-resolved BAT data of bursts: the empty squares mark the SGR 1627–41 events detected in 2008 May, and the grey data refer to the 2006 March ‘burst forest’ of SGR 1900+14 (Israel et al. 2008).

3.2 X-Ray Telescope data – persistent emission

The *Swift* XRT uses a CCD detector sensitive to photons with energies between 0.2 and 10 keV. Fourteen *Swift* observations of SGR 1627–41 were performed following the source re-activation. The XRT instrument was operated in photon counting (PC) mode. The first observation started about 4.6 h after the first burst was detected by the BAT. Table 2 reports the log of the XRT observations used for this work. The data were processed with standard procedures using the `FTOOLS` task `XRTPIPELINE` (version 0.11.6). We selected events with grades 0–12 and limited the analysis to the 0.3–10 keV range, where the PC response matrices are well calibrated.

The source was significantly detected in all observations with exposure time longer than 1 ks with the mean count rates given in Table 2. These values, corrected for the loss of counts caused by

Table 2. Journal of the 2008 *Swift*/XRT observations. The observation sequence number is composed of 00312579 followed by the three digit segment number given here (e.g. 00312579001).

Observation sequence number	Date (mm-dd)	Start/end time (UT) (hh:mm:ss)		Exposure ^a (ks)	Count rate (counts s ⁻¹)
001	05-28	12:58:14	13:31:27	2.0	0.067 ± 0.003
002	05-29	14:47:17	16:30:39	2.0	0.015 ± 0.003
003	05-30	11:35:15	14:58:56	1.9	0.010 ± 0.003
004	05-31	08:49:41	10:37:58	1.8	0.007 ± 0.002
005	06-01	05:32:11	07:34:56	2.0	0.008 ± 0.002
006	06-02	08:37:17	19:18:48	2.1	0.011 ± 0.003
007	06-06	10:35:23	12:16:30	0.6	<0.03 ^b
008	06-09	14:41:22	16:19:56	0.3	<0.03 ^b
009	06-12	13:07:43	16:35:58	1.9	0.006 ± 0.002
010	06-15	03:34:10	08:50:57	3.8	0.006 ± 0.002
011	06-18	16:54:48	20:24:56	2.3	0.010±0.002
012	06-21	18:46:38	23:39:55	5.2	0.008±0.002
013	07-02	05:17:00	17:10:56	1.5	0.005±0.002
014	07-05	15:29:07	21:59:57	5.6	0.005±0.001

^aThe exposure time is usually spread over several snapshots (single continuous pointings at the target) during each observation.

^bUpper limit at 3 σ confidence level (following Gehrels 1986).

hot columns and pixels (the correction factor was calculated with XRTMKARF), are plotted in Fig. 1 after conversion to flux as described below.

For the spectral analysis, we extracted the source events from a circular region with a radius of 20 pixel (1 pixel \simeq 2.37 arcsec), whereas the background events were extracted within an annular source-free region centred on SGR 1627–41 and with radii 50 and 75 pixel. Since individual data sets have too few counts for a meaningful spectral analysis, we extracted a cumulative spectrum. This corresponds to a total exposure of 32.9 ks and contains about 340 net counts in the 0.3–10 keV range. The data were rebinned with a minimum of 15 counts per energy bin. The ancillary response file was generated with XRTMKARF, and it accounts for different extraction regions, vignetting and point spread function corrections. We used the latest available spectral redistribution matrix (swxpc0to12s6_20010101v010.rmf). Adopting an absorbed power-law model, we find the following best-fitting parameters ($\chi_r^2 = 1.13$ for 21 d.o.f.): absorption $N_H = 10_{-3}^{+4} \times 10^{22}$ cm⁻² and photon index $\Gamma = 1.5_{-0.4}^{+0.7}$. We used the resulting observed 2–10 keV flux of $\sim 2.3 \times 10^{-12}$ erg cm⁻² s⁻¹ in order to derive the conversion factor 1 count s⁻¹ $\simeq 1.8 \times 10^{-10}$ erg cm⁻² s⁻¹.

Although the uncertainties in the spectral parameters are large, the *Swift*/XRT spectrum appears to be harder than the one observed by *XMM-Newton*/EPIC in 2008 February. To better investigate whether this hardening is statistically significant, we simultaneously fit the XRT and EPIC spectra with an absorbed power-law model with linked parameters and a free normalization factor. The resulting χ_r^2 (1.60 for 65 d.o.f.) is unacceptable, while an acceptable fit ($\chi_r^2 = 1.01$ for 64 d.o.f.) is obtained once the photon index is also left free to vary independently. The best-fitting parameters of the latter fit are: a common absorption of $N_H = (10_{-2}^{+1}) \times 10^{22}$ cm⁻² and photon indices $\Gamma_{XMM} = 3.5_{-0.5}^{+0.1}$ and $\Gamma_{XRT} = 1.5_{-0.5}^{+0.3}$ for the EPIC and XRT spectra, respectively.

4 DISCUSSION AND CONCLUSIONS

The recent, spectacular re-activation of SGR 1627–41, following a quiescent interval of nearly a decade, triggered the BAT instrument onboard *Swift* on 2008 May 28. Tens of bursts were observed, with

fluxes exceeding the underlying continuum by a factor of $> 10^5$. The bursts achieved a maximum luminosity of $\sim 10^{41}$ erg s⁻¹ and had a duration of < 0.5 s, typical of the bursts detected in SGRs. Thanks to the rapid response of *Swift*, the source was repeatedly observed with XRT in the days following the ‘burst forest’ emission, leading to the earliest post-burst observations ever obtained for this SGR. In fact, at the time of the previous active period, the persistent emission was observed only one month after the first burst detection (Woods et al. 1999).

With respect to the last pre-burst *XMM-Newton* observation, the source was detected in 2008 May and June at a much larger flux level (see Fig. 1) and with a considerably harder spectrum. A serendipitous *Chandra* observation performed only 20 h before the detection of the bursting activity provides a 3 σ upper limit on the absorbed flux of 5×10^{-12} erg cm⁻² s⁻¹ (0.5–10 keV band; Tiengo et al. 2008), showing that most of the flux enhancement occurred in less than a day. These facts indicate a significant phase transition marked by the burst activation. The correlated spectral hardening/flux increase is in line with what is observed in the long-term evolution of other magnetars (e.g. Mereghetti 2008), and expected in models in which the non-thermal X-ray emission is due to resonant up-scattering by magnetospheric currents (Thompson, Lyutikov & Kulkarni 2002).

The early flux decay of the source is shown in Fig. 4, where, for comparison, we also plot the flux of the decay that followed the past bursting activity of SGR 1627–41 and those of two AXPs, CXOU J164710.2–455216 (Israel et al. 2007) and 1E 2259+586 (Woods et al. 2004). The SGR 1627–41 data taken after more than two days from the 2008 May trigger are well fitted by a power-law decay (index ~ -0.2), but the XRT points at earlier times show a marked excess over this trend, indicating a very steep initial decay. This behaviour closely resembles that of 1E 2259+586: in that case, after the 2002 June bursts active phase, the source flux showed a double-component decay, with a steep component that decayed rapidly during the first ~ 2 d, followed by a slower year-long decay phase (Woods et al. 2004). Interestingly, the phase of steep flux decay (and harder spectra) was associated with a long-lasting period of bursting activity. This is consistent with what was observed in CXOU J164710.2–455216 and SGR 1627–41: in the former case, in which no steep/prompt decay was observed, the bursting activity

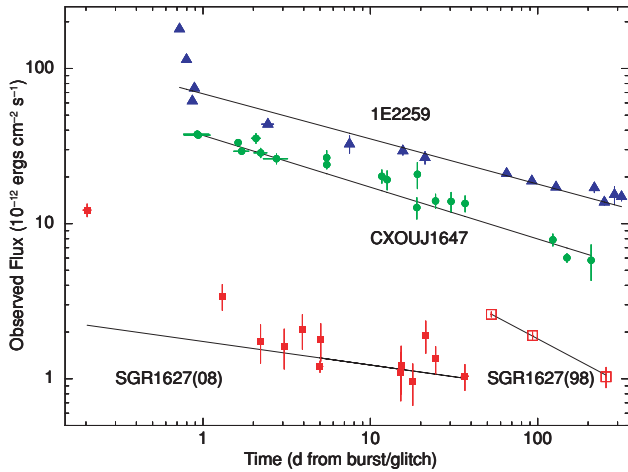


Figure 4. Comparison among flux decays of SGR 1627–41 (this work; Mereghetti et al. 2006; Woods et al. 2008b), CXOU J164710.2–455216 (Israel et al. 2007; filled circles) and 1E 2259+586 (Woods et al. 2004; filled triangles) following a period of burst emission and/or glitch. In the case of SGR 1627–41, we report the available data for both the 2008 (filled squares) and 1998 (open squares) activation periods. The solid lines represent the power-law best fits (see Section 4 for more details).

was already over at the time of the first observation of the persistent flux. In the latter case, after the activation of June 1998 only a shallow decay was monitored >60 d from the first bursts. The light curve of the recent SGR 1627–41 decay reveals both, the steep and shallow phase, and the last burst was detected by *Konus/Wind* between the first and the second XRT pointing (Golenetskii et al. 2008). The new observations support the presence of two distinct time-scales (a short, ~ 1 d, and a longer one, \sim month) in the flux decay following the outburst of a magnetar. In this respect, we notice that while a steep decay seems to point towards a magnetospheric effect (for instance, following current dissipation or other forms of activity), the decay index of the shallow phase ranges from about -0.6 (in the case of SGR 1627–41, 1998) to -0.2 (for 1E 2259+586 and SGR 1627–41, 2008) and is roughly compatible with crustal cooling (considering the uncertainties in the theoretical models, see Eichler et al. 2006, and references therein). The energetics and relative importance of the steep/shallow decay phases, nevertheless, greatly vary from source to source. Indeed, in some cases this requires a powering mechanism for the tail emission much more energetic than the burst energy deposition. This might be associated with magnetospheric current dissipation or crustal cooling following an impulsive heat deposition.

For several bursts, we had enough counts to perform a spectral analysis. The parameter values derived from the 2BB fits are in agreement with the results of a comprehensive analysis of a ‘burst forest’ emitted by SGR 1900+14 (Israel et al. 2008), which showed that the bursts populate almost homogeneously all temperatures between ~ 2 and ~ 12 keV, with a bimodal distribution behaviour and a sharp edge in the $kT-R^2$ plane. This supports the idea of two distinct emitting regions, a cold and larger one and a hot and smaller one, which, in turn, may be associated to the escaping regions of two populations of photons, from the O- and E- polarization modes. Interestingly, the bright bursts detected from SGR 1627–41 lie within the cloud of the SGR 1900+14 bursts (Fig. 3) and the luminosities of the two blackbody components are in agreement with the relation shown in fig. 6 of Israel et al. (2008), suggesting that short bursts form a continuum in terms of spectral properties, duration and

fluence. Finally, we notice that in the scenario proposed by Israel et al. (2008), the luminosity of the hot blackbody is not expected to exceed the magnetic Eddington luminosity (Thompson & Duncan 1995). In the case of SGR 1627–41, where the maximum luminosity observed by the BAT for the hot blackbody is $\sim 10^{41}$ erg s^{-1} , this translates into a lower limit for the magnetic field of $B > 1.8 \times 10^{14}$ G.

ACKNOWLEDGMENTS

This research is based on observations with the NASA/UK/ASI *Swift* mission. We thank the *Swift* duty scientists and science planners for making these observations possible. We also used data obtained with *XMM-Newton*, an ESA science mission with instruments and contributions directly funded by ESA Member States and NASA. The Italian authors acknowledge the partial support from ASI (ASI/INAF contracts I/088/06/0 and AAE TH-058). SZ and RLCS acknowledge support from STFC. NR is supported by an NWO Veni Fellowship. DG acknowledges the CNES for financial support.

REFERENCES

- Aptekar R. L., Frederiks D. D., Golenetskii S. V., Il’inskii V. N., Mazets E. P., Pal’shin V. D., Butterworth P. S., Cline T. L., 2001, *ApJS*, 137, 227
 Barthelmy S. D. et al., 2005, *Space Sci. Rev.*, 120, 143
 Burrows D. N. et al., 2005, *Space Sci. Rev.*, 120, 165
 Corbel S., Chapuis C., Dame T. M., Durouchoux P., 1999, *ApJ*, 526, L29
 Eichler D., Lyubarsky Y., Kouveliotou C., Wilson C. A., 2006, preprint (astro-ph/0611747)
 Feroci M., Costa E., Amati L., Piro L., Martino B., di Ciolo L., Coletta A., Frontera F., 1998, *IAU Circ.*, 6945, 3
 Feroci M., Caliendo G. A., Massaro E., Mereghetti S., Woods P. M., 2004, *ApJ*, 612, 408
 Gehrels N., 1986, *ApJ*, 303, 336
 Gehrels N. et al., 2004, *ApJ*, 611, 1005
 Golenetskii S., Aptekar R., Mazets E., Pal’shin V., Frederiks D., Oleynik P., Ulanov M., Cline T., 2008, *GCN Circ.*, 7778
 Hurley K., Kouveliotou C., Woods P., Mazets E., Golenetskii S., Frederiks D. D., Cline T., van Paradijs J., 1999, *ApJ*, 519, L143
 Israel G. L., Campana S., Dall’Osso S., Muno M. P., Cummings J., Perna R., Stella L., 2007, *ApJ*, 664, 448
 Israel G. L. et al., 2008, *ApJ*, in press
 Jansen F. et al., 2001, *A&A*, 365, L1
 Kouveliotou C., Kippen M., Woods P., Richardson G., Connaughton V., McCollough M., 1998, *IAU Circ.*, 6944, 2
 Kouveliotou C. et al., 2003, *ApJ*, 596, L79
 Mazets E. P. et al., 1999, *ApJ*, 519, L151
 Mereghetti S., 2008, *A&AR*, 15, 225
 Mereghetti S. et al., 2006, *A&A*, 450, 759
 Nakagawa Y. E. et al., 2007, *PASJ*, 59, 653
 Olive J.-F. et al., 2004, *ApJ*, 616, 1148
 Palmer D. et al., 2008, *GCN Circ.*, 7777
 Roming P. W. A. et al., 2005, *Space Sci. Rev.*, 120, 95
 Smith D. A., Bradt H. V., Levine A. M., 1999, *ApJ*, 519, L147
 Thompson C., Duncan R. C., 1995, *MNRAS*, 275, 255
 Thompson C., Lyutikov M., Kulkarni S. R., 2002, *ApJ*, 574, 332
 Tiengo A. et al., 2008, *Astron. Tel.*, 1559
 Wachter S. et al., 2004, *ApJ*, 615, 887
 Woods P. M. et al., 1999, *ApJ*, 519, L139
 Woods P. M. et al., 2004, *ApJ*, 605, 378
 Woods P. M., Kouveliotou C., Göğüş E., Hurley K., 2008a, *Astron. Tel.*, 1549
 Woods P. M., Kouveliotou C., Göğüş E., Hurley K., Tomsick J., 2008b, *Astron. Tel.*, 1564

This paper has been typeset from a $\text{\TeX}/\text{\LaTeX}$ file prepared by the author.